

CONSISTENT VIDEO-TO-VIDEO TRANSFER USING SYNTHETIC DATASET

Jiaxin Cheng, Tianjun Xiao & Tong He

Amazon Web Services Shanghai AI Lab

{cjiaxin,tianjux,htong}@amazon.com

ABSTRACT

We introduce a novel and efficient approach for text-based video-to-video editing that eliminates the need for resource-intensive per-video-per-model finetuning. At the core of our approach is a synthetic paired video dataset tailored for video-to-video transfer tasks. Inspired by Instruct Pix2Pix’s image transfer via editing instruction, we adapt this paradigm to the video domain. Extending the Prompt-to-Prompt to videos, we efficiently generate paired samples, each with an input video and its edited counterpart. Alongside this, we introduce the Long Video Sampling Correction during sampling, ensuring consistent long videos across batches. Our method surpasses current methods like Tune-A-Video, heralding substantial progress in text-based video-to-video editing and suggesting exciting avenues for further exploration and deployment. <https://github.com/amazon-science/instruct-video-to-video/tree/main>

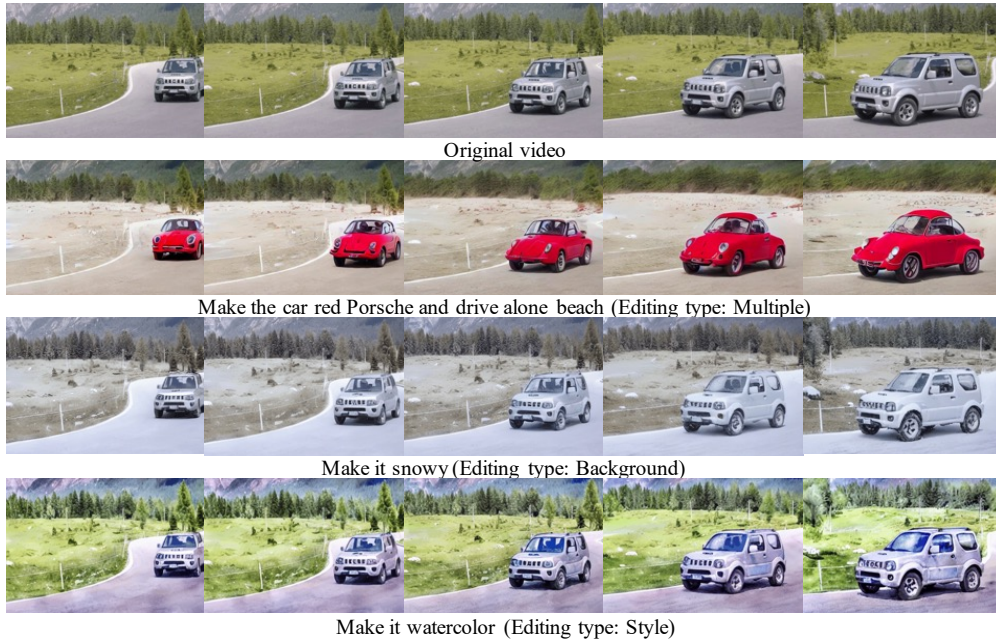


Figure 1: InsV2V has versatile editing capabilities encompassing background, object, and stylistic changing. Our method adopts a one-model-all-video strategy, achieving comparable performance while necessitating only inference. InsV2V eliminates the need to specify prompts for both original and target videos, simplifying the process by requiring only an edit prompt, thereby enhancing intuitiveness in video editing.

1 INTRODUCTION

Text-based video editing Wu et al. (2022); Zhao et al. (2023); Wang et al. (2023a); Qi et al. (2023); Liu et al. (2023) has recently garnered significant interest as a versatile tool for multimedia content manipulation. However, existing approaches present several limitations that undermine their practical utility. Firstly, traditional methods typically require per-video-per-model finetuning, which imposes a considerable computational burden. Furthermore, current methods require users to describe both the original and the target video Wu et al. (2022); Zhao et al. (2023); Wang et al. (2023a); Qi et al. (2023); Liu et al. (2023). This requirement is counterintuitive, as users generally only want to specify what edits they desire, rather than providing a comprehensive description of the original content. Moreover, these methods are constrained to individual video clips; if a video is too long to fit into model, these approaches fail to ensure transfer consistency across different clips.

To overcome these limitations, we introduce a novel method with several distinctive features. Firstly, our approach offers a universal one-model-all-video transfer, freeing the process from per-video-per-model finetuning. Moreover, our model simplifies user interaction by only necessitating an intuitive editing prompt, rather than detailed descriptions of both the original and target videos, to carry out desired alterations. Secondly, we develop a synthetic dataset precisely crafted for video-to-video transfer tasks. Through rigorous pairing of text and video components, we establish an ideal training foundation for our models. Lastly, we introduce a sampling method specifically tailored for generating longer videos. By using the transferred results from preceding batches as a reference, we achieve consistent transfers across extended video sequences.

We introduce Instruct Video-to-Video (InsV2V), a diffusion-based model that enables video editing using only an editing instruction, eliminating the need for per-video-per-model tuning. This capability is inspired by Instruct Pix2Pix Brooks et al. (2023), which similarly allows for arbitrary image editing through textual instructions. A significant challenge in training such a model is the scarcity of naturally occurring paired video samples that can reflect an editing instruction. Such video pairs are virtually nonexistent in the wild, motivating us to create a synthetic dataset for training.

Our synthetic video generation pipeline builds upon a large language model (LLM) and the Prompt-to-Prompt Hertz et al. (2022) method that is initially designed for image editing tasks (Figure 2). We use an example-driven in-context learning approach to guide the LLM to produce these paired video descriptions. Additionally, we adapt the Prompt-to-Prompt (PTP) method to the video domain by substituting the image diffusion model with a video counterpart Ho et al. (2022c). This modification enables the generation of paired samples that consist of an input video and its edited version, precisely reflecting the relationships delineated by the editing prompts.

In addressing the limitations of long video editing in conventional video editing methods, we introduce Long Video Sampling Correction (LVSC). This technique mitigates challenges arising from fixed frame limitations and ensures seamless transitions between separately processed batches of a lengthy video. LVSC employs the final frames of the previous batch as a reference to guide the generation of subsequent batches, thereby maintaining visual consistency across the entire video. We also tackle issues related to global or holistic camera motion by introducing a motion compensation feature that uses optical flow. Our empirical evaluations confirm the effectiveness of LVSC and motion compensation in enhancing video quality and consistency.

2 RELATED WORK

Diffusion Models The advent of the diffusion model Sohl-Dickstein et al. (2015); Ho et al. (2020) has spurred significant advancements in the field of image generation. Over the course of just a few years, we have observed the diffusion model making groundbreaking progress in a variety of fields. This includes areas such as super-resolution Saharia et al. (2022c), colorization Saharia et al. (2022a), novel view synthesis Watson et al. (2022), style transfer Zhang et al. (2023), and 3D generation Poole et al. (2022); Tang et al. (2023); Cheng et al. (2023b). These breakthroughs have been achieved through various means. Some are attributable to the enhancements in network structures such as Latent Diffusion Models (also known as Stable Diffusion) Rombach et al. (2022), GLIDE Nichol et al. (2022), DALLE2 Ramesh et al. (2022), SDXL Podell et al. (2023), and Imagen Saharia et al. (2022b). Others are a result of improvements made in the training paradigm Nichol & Dhariwal (2021); Song & Ermon (2019); Dhariwal & Nichol (2021); Song et al. (2020b;a). Fur-

thermore, the ability to incorporate various conditions during image generation has played a crucial role. These conditions include elements such as layout Cheng et al. (2023a); Rombach et al. (2022), segmentation Avrahami et al. (2023; 2022); Balaji et al. (2022); Yang et al. (2023a), or even the use of an image as reference Mou et al. (2023); Ruiz et al. (2023); Gal et al. (2022).

Diffusion-based Text-Guided Image Editing Image editing is a process where we don’t desire completely unconstrained generation but modifying an image under certain guidance (*i.e.* a reference image) during its generation. Various methods have been proposed to address this task. Simple zero-shot image-to-image translation methods, such as SDEdit Meng et al. (2021) performed through diffusion and denoising on reference image. Techniques that incorporate a degree of optimization, such as Imagic Kawar et al. (2023), which utilizes the concept of textual inversion Gal et al. (2022), and Null-text Inversion Mokady et al. (2023), which leverages the Prompt-to-Prompt strategy Hertz et al. (2022) to control the behavior of cross-attention in the diffusion model for editing, have also been explored. These methods can impede the speed of editing due to the necessity for per-image-per-optimization. Models like Instruct Pix2Pix Brooks et al. (2023) have been employed to achieve image editing by training on synthetic data. This approach adeptly balances editing capabilities and fidelity to the reference image.

Diffusion-based Text-Guided Video Editing The success of the diffusion model in image generation has been extended to video generation as well Ho et al. (2022b); Harvey et al. (2022); Blattmann et al. (2023); Mei & Patel (2023); Ho et al. (2022a), and similarly, text-guided video editing has sparked interest within the community. Techniques akin to those in image editing have found applications in video editing. For instance, Dreamix Molad et al. (2023) uses diffusion and denoising for video editing, reminiscent of the approach in SDEdit Meng et al. (2021). Strategies altering the behavior of the cross-attention layer to achieve editing, like the Prompt-to-Prompt Hertz et al. (2022), have been adopted by methods such as Vid2Vid-Zero Wang et al. (2023a), FateZero Qi et al. (2023), and Video-p2p Liu et al. (2023). Recent developments Wang et al. (2023b); Esser et al. (2023); Zhao et al. (2023) leverage certain condition modalities extracted from the original video, like depth maps or edge sketches, to condition the video generation. The related, albeit non-diffusion-based, method Text2live Bar-Tal et al. (2022) also provides valuable perspectives on video editing.

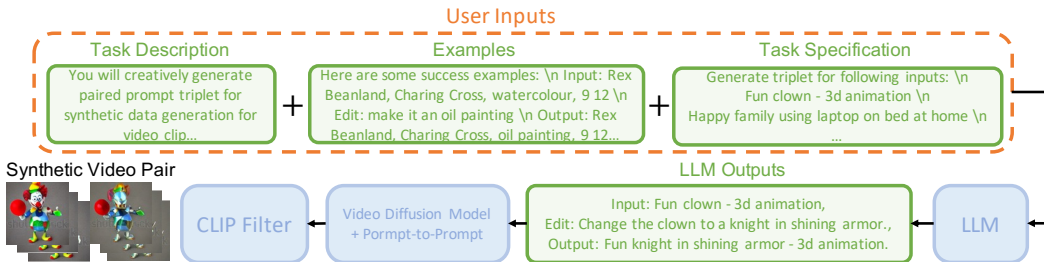


Figure 2: The pipeline for generating a synthetic dataset using a large language model, whose outputs include the prompt triplet consisting of input, edit, and edited prompts, as well as a corresponding pair of videos. Visualization of generated videos can be found in Appendix B

3 SYNTHETIC PAIRED VIDEO DATASET

A crucial element for training a model capable of arbitrary video-to-video transfer, as opposed to a per-video-per-model approach, lies in the availability of ample paired training data. Each pair consists of an input video and its corresponding edited version, providing the model with a diverse range of examples essential for generalized performance. However, the scarcity of naturally occurring video pairs with such correspondence poses a significant challenge to the training process.

To address this, we introduce the concept of a trade-off between initial training costs, including dataset creation, and long-term efficiency. We advocate for the use of synthetic data, which, while incurring an upfront cost, accurately maintains the required correspondence and fulfills the conditions for effective video-to-video transfer learning. The merit of this synthetic data generation approach is underscored by its potential to offset the initial investment through substantial time savings and efficiency in the subsequent inference stages. This approach contrasts with ‘per-vid-

per-model’ methods that necessitate repetitive fine-tuning for each new video, making our strategy both cost-effective and practical in diverse real-world applications.

The potential of synthetic data generation, well-documented in the realm of text-guided editing Brooks et al. (2023), is thereby extended to video-to-video transfer. This method allows us to construct the optimal conditions for the model to learn, offering a practical solution to the inherent obstacles associated with acquiring matching real-world video pairs.

3.1 DATASET CREATION:

In order to generate the synthetic dataset, we leverage the approach of Prompt-to-Prompt (PTP) Hertz et al. (2022), a proven method for producing paired samples in the field of image editing. The PTP employs both self-attention and cross-attention replacements to generate semantically aligned edited images. In self-attention, the post-softmax probability matrix of the input prompt replaces that of the edited prompt. The cross-attention replacement specifically swaps the text embedding of the edited prompt with that of the input prompt.

In the context of video-to-video transfer, we adapt PTP by substituting its underlying image diffusion models with a video diffusion model. In addition, we extend the self-attention replacement to temporal attention layers, a critical modification for maintaining structural coherence between input and edited videos. Figure 2 shows the overall pipeline for data generation. To guide the synthetic data generation, we employ a set of paired text prompts, comprising an input prompt, an edited prompt, and an edit prompt. The input prompt corresponds to the synthetic original video, while the edited prompt and the edit prompt represent the desired synthetic edited video and the specific changes to be applied on the original video respectively.

3.2 PROMPT SOURCES

Our synthetic dataset is constructed using paired prompts from two differentiated sources, each serving a specific purpose in the training process. The first source, LAION-IPTP, employs a fine-tuned GPT-3 model to generate prompts based on 700 manually labeled captions from the LAION-Aesthetics dataset Brooks et al. (2023). This yielded a set of 450,000 prompt pairs, of which 304,168 were utilized for synthetic video creation. While the GPT-3-based prompts offer a substantial volume of data, they originate from image captions and thus have limitations in their applicability to video generation. This led us to incorporate a second source, WebVid-MPT, which leverages video-specific captions from the WebVid 10M dataset Bain et al. (2021). Using MPT-30B Team (2023) in a zero-shot manner, we devised a set of guidelines (see Appendix A for details) to generate the needed paired prompts, adding an additional 100,000 samples to our dataset. Crucially, the WebVid-MPT source yielded a threefold increase in the success rate of generating usable samples compared to the LAION-IPTP source after sample filtering, reinforcing the need for video-specific captions in the training process. The LAION-IPTP prompt source demonstrated a success rate of 5.49% (33,421 successful generations from 608,336 attempts). The WebVid-MPT prompt source showed a higher success rate of 17.49% (34,989 successful generations from 200,000 attempts).

3.3 IMPLEMENTATION DETAILS AND SAMPLE SELECTION CRITERIA

Implementation Details: We use public available text-to-video model¹ for generating synthetic videos. Each video has 16 frames, processed over 30 DDIM Song et al. (2020a) steps by the diffusion model. The self-attention and cross-attention replacements in the Prompt-to-Prompt model terminate at a random step within the ranges of 0.3 to 0.45 and 0.6 to 0.85 respectively (out of 30 steps). The classifier-free guidance scale is a random integer value between 5 and 12.

Sample Selection Criteria: To ensure the quality of our synthetic dataset, we employ a CLIP-based filtering. For each prompt, generation is attempted with two random seeds, and three distinct clip scores are computed: CLIP Text Score: Evaluates the cosine similarity between each frame and the text. CLIP Frame Score: Measures the similarity between original and edited frames. CLIP Direction Score: Quantifies the similarity between the transition of original-frame-to-edited-frame and original-text-to-edited-text. These scores are obtained for each of the 16 frames and averaged.

¹<https://modelscope.cn/models/damo/text-to-video-synthesis/summary>

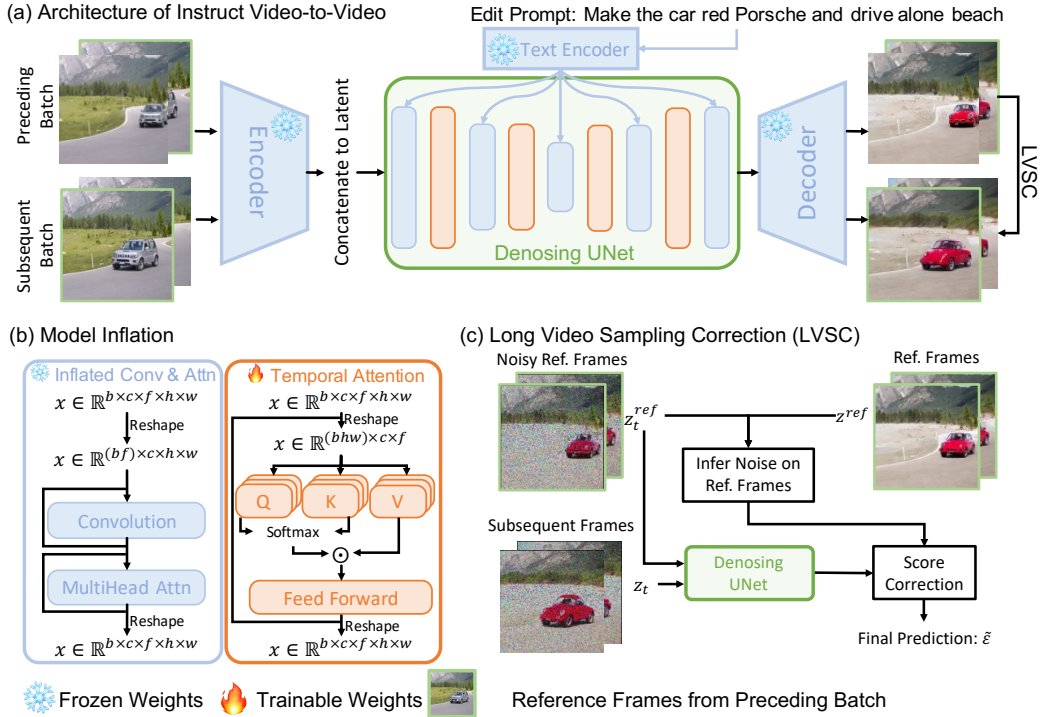


Figure 3: (a) The architecture of InsV2V. For handling long videos processed in multiple batches, our approach leverages the proposed LVSC to utilize the final frames from the preceding batch as reference frames for the subsequent batch. (b) The inflated convolutionals and attention layer, as well as temporal attention layer can handle 5D video tensors by dynamically reshaping them. (c) During each denoising iteration, the LVSC adjusts the predicted noise $\tilde{\epsilon}_\theta(z_t)$ based on reference frames z_t^{ref} prior to executing the DDIM denoising.

A sample is preserved if it meets the following conditions: CLIP Text Score > 0.2 for both original and edited videos, CLIP Direction Score > 0.2 , and CLIP Frame Score > 0.5 . Samples that fail to meet these criteria are discarded.

4 MODEL ARCHITECTURE

4.1 PRELIMINARIES

Diffusion models learn to predict content in an image by iteratively denoising an entirely random Gaussian noise. In the training process, the input image is first corrupted by the Gaussian noise, termed diffusion. The model’s task is to restore a diffused noisy image to its original form. This process can be considered as the optimization of the variational lower bound on the distribution $p(x)$ of the image x with a T step Markovian inverse process. Various conditions c , such as text, images, and layouts, can be incorporated into diffusion models during the learning process. The model ε_θ we aim to train is conditioned on text and its training loss can be expressed as

$$L = \mathbb{E}_{x, \varepsilon \sim \mathcal{N}(0,1), t} \|\varepsilon - \varepsilon_\theta(x_t, t, c)\|^2 \quad (1)$$

Where x_t is the result of diffusing the input image x at timestep $t \in [1, T]$ using random noise ε . In practice, we employ the Latent Diffusion Model (LDM) Rombach et al. (2022) as our backbone model and condition it on input videos by concatenating the videos to the latent space, as illustrated in Figure 3 (a). Instead of generating images in the RGB pixel space, LDM employs a trained Vector Quantized Variational AutoEncoder (VQVAE) Esser et al. (2021) to convert images to visual codes in latent space. This allows the model to achieve better results with the same training resources.

Specifically, the image x is first transformed into a latent code $z = \text{VQEnc}(x)$, and the model learns to predict $p(z)$ from random noise. In the context of the video editing, two distinct conditions exist: the editing instructions and the reference video, represented by c_T and c_V respectively. The model is designed to predict $p(z)$ by optimizing the following loss function:

$$L = \mathbb{E}_{\text{VQEnc}(x), \varepsilon \sim \mathcal{N}(0,1), t} \|\varepsilon - \varepsilon_\theta(z_t, t, c_V, c_T)\|^2 \quad (2)$$

4.2 INFLATE IMAGE-TO-IMAGE MODEL TO VIDEO-TO-VIDEO MODEL

Given the substantial similarities between image-to-image transfer and video-to-video transfer, our model utilizes a foundational pre-trained 2D image-to-image transfer diffusion model. Using foundational model simplifies training but falls short in generating consistent videos, causing noticeable jitter when sampling frames individually. Thus, we transform this image-focused model into a video-compatible one for consistent frame production. We adopt model inflation as recommended in previous studies Wu et al. (2022); Guo et al. (2023). This method modifies the single image diffusion model to produce videos. The model now accepts a 5D tensor input $x \in \mathbb{R}^{b \times c \times f \times h \times w}$. Given its architecture was designed for a 4D input, we adjust the convolutional and attention layers in the model (Figure 3 (b)). Our inflation process involves: (1) Adapting convolutional and attention layers to process a 5D tensor by reshaping it temporarily to 4D. Once processed, it’s reverted to 5D. (2) Introducing temporal attention layers for frame consistency. When these layers handle a 5D tensor, they reshape it to a 3D format, enabling pixel information exchange between frames via attention.

4.3 SAMPLING

During sampling, we employ an extrapolation technique named Classifier-Free Guidance (CFG) Ho & Salimans (2022) to augment the generation quality. Given that we have two conditions, namely the conditional video and the editing prompt, we utilize the CFG method for these two conditions as proposed in Brooks et al. (2023). Specifically, for each denoising timestep, three predictions are made under different conditions: the unconditional inference $\varepsilon_\theta(z_t, \emptyset, \emptyset)$, where both the conditions are an empty string and an all-zero video; the video-conditioned prediction $\varepsilon_\theta(z_t, c_V, \emptyset)$; and the video and prompt-conditioned prediction $\varepsilon_\theta(z_t, c_V, c_T)$. Here, we omit timestep t for symbolic convenience. The final prediction is an extrapolation between these three predictions with video and text classifier-free guidance scale $s_V \geq 1$ and $s_T \geq 1$.

$$\begin{aligned} \tilde{\varepsilon}_\theta(z_t, c_V, c_T) &= \varepsilon_\theta(z_t, \emptyset, \emptyset) \\ &+ s_V \cdot (\varepsilon_\theta(z_t, c_V, \emptyset) - \varepsilon_\theta(z_t, \emptyset, \emptyset)) \\ &+ s_T \cdot (\varepsilon_\theta(z_t, c_V, c_T) - \varepsilon_\theta(z_t, c_V, \emptyset)) \end{aligned} \quad (3)$$

4.4 LONG VIDEO SAMPLING CORRECTION FOR EDITING LONG VIDEOS

In video editing, models often face limitations in processing extended video lengths in one go. Altering the number of input frames can compromise the model’s efficacy, as frame count is usually preset during training. To manage lengthy videos, we split them into smaller batches for independent sampling. While intra-batch frame consistency is preserved, inter-batch consistency isn’t guaranteed, potentially resulting in visible discontinuities at batch transition points.

To address this issue, we propose Long Video Sampling Correction (LVSC): during sampling, the results from the final N frames of the previous video batch can be used as a reference to guide the generation of the next batch (Figure 3 (c)). This technique helps to maintain visual consistency across different batches. Specifically, let $z^{ref} = z_0^{prev}[:, -N :] \in \mathbb{R}^{1, N, c, h, w}$ denote the last N frames from the transfer result of the previous batch. Here, to avoid confusion with the batch size, we set the batch size to 1. The ensuing batch is the concatenation of noisy reference frames and subsequent frames $[z_t^{ref}, z_t]$. On the model’s prediction $\varepsilon_\theta(z_t) := \varepsilon_\theta(z_t, t, c_V, c_T)$, we implement a score correction and the final prediction is the summation between raw prediction $\varepsilon_\theta(z_t)$ and correction term $\varepsilon_t^{ref} - \varepsilon_\theta(z_t^{ref})$, where ε_t^{ref} is the closed-form inferred noise on reference frames. For notation simplicity, we use $\varepsilon(z_t^{ref})$ and $\varepsilon(z_t)$ to denote the model’s predictions on reference and subsequent frames, though they are processed together by the model instead of separate inputs.

$$\varepsilon_t^{ref} = \frac{z_t^{ref} - \sqrt{\bar{\alpha}_t} z_0}{\sqrt{1 - \bar{\alpha}_t}} \in \mathbb{R}^{1, N, c, h, w} \quad (4)$$

$$\tilde{\varepsilon}_\theta(z_t) = \varepsilon_\theta(z_t) + \frac{1}{N} \sum_{i=1}^N (\varepsilon_t^{ref}[:, i] - \varepsilon_\theta(z_t^{ref})[:, i]) \quad (5)$$

We apply averaging on the correction term when there are multiple reference frames as shown in Equations (4) and (5), where $\bar{\alpha}_t$ is the diffusion coefficient for timestep t (*i.e.* $z_t = \mathcal{N}(\sqrt{\bar{\alpha}_t} z_0, (1 - \bar{\alpha}_t)I)$). In our empirical observations, we find that when the video has global or holistic camera motion, the score correction may struggle to produce consistent transfer results. To address this issue, we additionally introduce a motion compensation that leverages optical flow to establish correspondences between each pair of reference frames and the remaining frames in the batch. We then warp the score correction in accordance with this optical flow with details presented in Appendix D.

5 EXPERIMENTS

5.1 EXPERIMENTAL SETUP

Dataset For our evaluation, we used the Text-Guided Video Editing (TGVE) competition dataset². The TGVE dataset contains 76 videos that come from three different sources: Videov, Youtube, and DAVIS Perazzi et al. (2016). Every video in the dataset comes with one original prompt that describes the video and four prompts that suggest different edits for each video. Three editing prompts pertain to modifications in *style*, *background*, or *object* within the video. Additionally, a *multiple* editing prompt is provided that may incorporate aspects of all three types of edits simultaneously.

Metrics for Evaluation Given that our focus is on text-based video editing, we look at three critical aspects. First, we assess whether the edited video accurately reflects the editing instructions. Second, we determine whether the edited video successfully preserves the overall structure of the original video. Finally, we consider the aesthetics of the edited video, ensuring it is free of imperfections such as jittering. Our evaluation is based on user study and automated scoring metrics. In the user study, we follow TGVE competition to ask users three key questions. The **Text Alignment** question: Which video better aligns with the provided caption? The **Structure** question: Which video better retains the structure of the input video? The **Quality** question: Aesthetically, which video is superior? These questions aim to evaluate the quality of video editing, focusing on the video’s alignment with editing instructions, its preservation of the original structure, and its aesthetic integrity. For objective metrics, we incorporate PickScore Kirstain et al. (2023) that computes the average image-text alignment over all video frames and CLIP Frame (Frame Consistency) Radford et al. (2021), which measures the average cosine similarity among CLIP image embeddings across all video frames. We prefer PickScore over the CLIP text-image score since it’s tailored to more closely align with human perception of image quality, which is also noticed by Podell et al. (2023).

5.2 BASELINE METHODS

We benchmark InsV2V against leading text-driven video editing techniques: Tune-A-Video Wu et al. (2022), Vid2Vid-Zero Wang et al. (2023a), Video-P2P Liu et al. (2023), and ControlVideo Zhao et al. (2023). Tune-A-Video has been treated as a *de facto* baseline in this domain. Vid2Vid-Zero and Video-P2P adopt the cross-attention from Prompt-to-Prompt (PTP) Hertz et al. (2022), while ControlVideo leverages ControlNet Zhang & Agrawala (2023). We test all methods for 32 frames, but PTP-based ones, due to their computational demand, are limited to 8 frames. Baselines are processed in a single batch to avoid inter-batch inconsistencies and use latent inversion Mokady et al. (2023) for structure preservation, which causes double inference time. Conversely, our method retains the video’s structure more efficiently.

We also extend the comparison to include recent tuning-free video editing methods such as Token-Flow Geyer et al. (2023), Render-A-Video Yang et al. (2023b), and Pix2Video Ceylan et al. (2023).

²<https://sites.google.com/view/loveucvpr23/track4>

These methods, by eliminating the necessity for individual video model tuning, present a comparable benchmark to our approach. To ensure frame-to-frame consistency, these methods either adopt cross-frame attention similar to Tune-A-VideoWu et al. (2022), as seen in Ceylan et al. (2023); Yang et al. (2023b), or establish pixel-level correspondences between features and a reference key frame as in Geyer et al. (2023). This approach is effective in maintaining quality when there are minor scene changes. However, in scenarios with significant differences between the key and reference frames, these methods may experience considerable degradation in video quality. This limitation is more clearly illustrated in Figure 12 in the Appendix.

5.3 MODEL DETAILS

Our model is adapted from a single image editing Stable Diffusion Brooks et al. (2023) and we insert temporal attention modules after each spatial attention layers as suggested by Guo et al. (2023). Our training procedure makes use of the Adam optimizer with a learning rate set at 5×10^{-5} . The model is trained with a batch size of 512 over a span of 2,000 iterations. This training process takes approximately 30 hours to complete on four NVIDIA A10G GPUs.

During sampling, we experiment with varying hyperparameters for video classifier-free guidance (VCFG) within the choice of [1.2, 1.5, 1.8], text classifier-free guidance to 10 and video resolutions of 256 and 384. A detailed visual comparison using these differing hyperparameters can be found in the supplementary material (Appendix E). The hyperparameters combination that achieves the highest PickScore is selected as the final sampling result. Each video is processed in three distinct batches using LVSC with a fixed frame count of 16 within a batch, including reference frames from preceding batch, and resulting in a total frame count of 32.

5.4 LONG VIDEO SCORE CORRECTION AND MOTION COMPENSATION

Table 1: Comparison of motion-aware MSE and CLIP frame similarity between the last frame of the preceding batch and the first frame of the subsequent batch on TGVE dataset.

LVSC	MC	MAMSE (%) ↓	CLIPFrame ↑
✗	✗	2.02	0.9072
✓	✗	1.44	0.9093
✓	✓	1.37	0.9095

To assess performance improvement, we employ CLIP Frame Similarity and Motion-Aware Mean Squared Error (MAMSE) as evaluation metrics. Unlike traditional MSE, MAMSE accounts for frame-to-frame motion by utilizing optical flow to warp images, thereby ensuring loss computation in corresponding regions. Incorporating Long Video Score Correction (LVSC) and Motion Compensation (MC)

has led to enhanced performance as reflected in Table 1. Further qualitative comparison, detailing the benefits of LVSC and MC, are provided in Appendices C and D.

5.5 USER STUDY

Table 2: The first two columns display automated metrics concerning CLIP frame consistency and PickScore. The final four columns pertain to a user study conducted under the TGVE protocol, where users were asked to select their preferred video when comparing the method against the TAV.

Method	CLIPFrame	PickScore	Text Alignment	Structure	Quality	Average
TAV*	0.924	20.36	-	-	-	-
CAMP*	0.899	20.71	0.689	0.486	0.599	0.591
T2L_HERO*	0.923	20.22	0.531	0.601	0.564	0.565
Vid2Vid-Zero	0.926	20.35	0.400	0.357	0.560	0.439
Video-P2P	0.935	20.08	0.355	0.534	0.536	0.475
ControlVideo	0.930	20.06	0.328	0.557	0.560	0.482
TokenFlow	0.940	20.49	0.287	0.563	0.624	0.491
Pix2Video	0.916	20.12	0.468	0.529	0.538	0.511
Render-A-Video	0.909	19.58	0.326	0.551	0.525	0.467
InsV2V (Ours)	0.911	20.76	0.690	0.717	0.689	0.699

*: Scores from TGVE leaderboard.

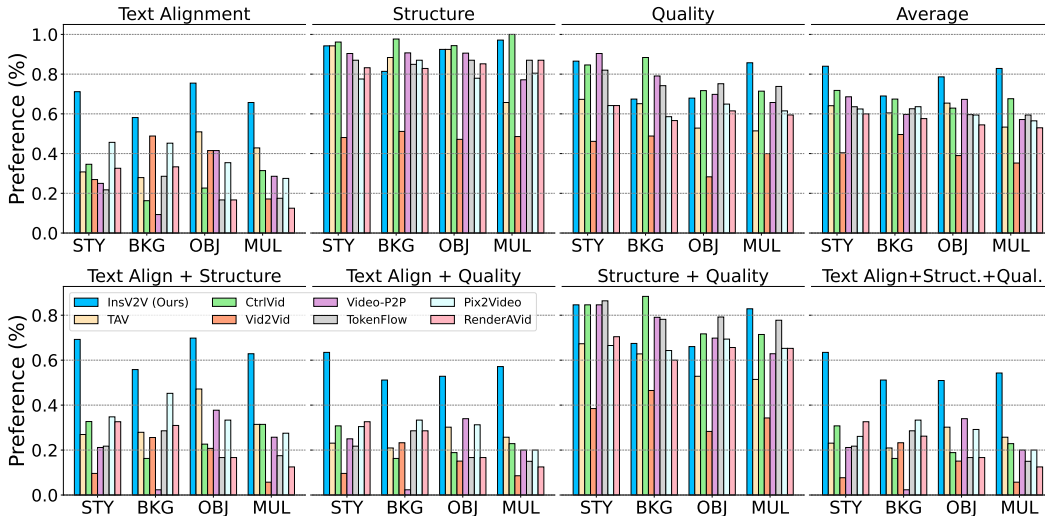


Figure 4: The abbreviations on x-axis indicate user preferences across four types of video editing within TGVE: Style, Background, Object, and Multiple. Each title specifies the evaluation metrics used for the corresponding figures. A "+" symbol signifies that the user vote meets multiple criteria. Additional qualitative results are presented in Appendix F

We conducted two separate user studies. The first followed the TGVE protocol, where we used Tune-A-Video as the baseline and compared the outcomes of our method with this well-known approach. However, we realized that this method of always asking users to choose a better option might not fully represent the reality, where both videos could either perform well or poorly. Thus, in the second user study, we compare our method with seven publicly available baselines. Instead of asking users to choose a better video, we asked them to vote for the quality of text alignment, structural preservation, and aesthetic quality for each transferred video. As evidenced by Table 2 and Figure 4, our approach excelled in all metrics except CLIP Frame similarity. We contend that CLIP Frame similarity is not an entirely apt metric because it only captures semantic similarity between individual frames, which may not be constant throughout a well-edited video due to changing scenes.

In our evaluation protocol, we additionally introduce a multi-metric assessment, capturing cases where videos satisfy multiple evaluation criteria concurrently. This composite measure addresses a key shortcoming of single metrics, which may inadequately reflect overall editing performance. For example, a high structure score might indicate that the edited video perfectly preserves the original, but such preservation could come at the expense of alignment with the editing instruction.

The results presented in Figure 4 further corroborate the advantages of our approach. While baseline methods demonstrate respectable performance when text alignment is not a prioritized criterion, they fall short when this element is incorporated into the assessment. In contrast, our method not only excels in aligning the edited video with the textual instructions but also maintains the structural integrity of the video, resulting in a high-quality output. This dual success underlines the robustness of our method in meeting the nuanced requirements of video editing tasks.

6 CONCLUSION

This research tackles the problem of text-based video editing. We have proposed a synthetic video generation pipeline, capable of producing paired data required for video editing. To adapt to the requirements of video editing, we have employed the model inflation technique to transform a single image diffusion model into a video diffusion model. As an innovation, we've introduced the Long Video Sampling Correction to ensure the generation of consistent long videos. Our approach is not only efficient but also highly effective. The user study conducted to evaluate the performance of our model yielded very high scores, substantiating the robustness and usability of our method in real-world applications.

REFERENCES

- Omri Avrahami, Dani Lischinski, and Ohad Fried. Blended diffusion for text-driven editing of natural images. In *Proceedings of the IEEE/CVF Conference on Computer Vision and Pattern Recognition*, pp. 18208–18218, 2022.
- Omri Avrahami, Thomas Hayes, Oran Gafni, Sonal Gupta, Yaniv Taigman, Devi Parikh, Dani Lischinski, Ohad Fried, and Xi Yin. Spatext: Spatio-textual representation for controllable image generation. In *Proceedings of the IEEE/CVF Conference on Computer Vision and Pattern Recognition*, pp. 18370–18380, 2023.
- Max Bain, Arsha Nagrani, Gül Varol, and Andrew Zisserman. Frozen in time: A joint video and image encoder for end-to-end retrieval. In *IEEE International Conference on Computer Vision*, 2021.
- Yogesh Balaji, Seungjun Nah, Xun Huang, Arash Vahdat, Jiaming Song, Karsten Kreis, Miika Aittala, Timo Aila, Samuli Laine, Bryan Catanzaro, et al. ediffi: Text-to-image diffusion models with an ensemble of expert denoisers. *arXiv preprint arXiv:2211.01324*, 2022.
- Omer Bar-Tal, Dolev Ofri-Amar, Rafail Fridman, Yoni Kasten, and Tali Dekel. Text2live: Text-driven layered image and video editing. In *European conference on computer vision*, pp. 707–723. Springer, 2022.
- Andreas Blattmann, Robin Rombach, Huan Ling, Tim Dockhorn, Seung Wook Kim, Sanja Fidler, and Karsten Kreis. Align your latents: High-resolution video synthesis with latent diffusion models. In *Proceedings of the IEEE/CVF Conference on Computer Vision and Pattern Recognition*, pp. 22563–22575, 2023.
- Tim Brooks, Aleksander Holynski, and Alexei A Efros. Instructpix2pix: Learning to follow image editing instructions. In *CVPR*, pp. 18392–18402, 2023.
- Duygu Ceylan, Chun-Hao P Huang, and Niloy J Mitra. Pix2video: Video editing using image diffusion. In *Proceedings of the IEEE/CVF International Conference on Computer Vision*, pp. 23206–23217, 2023.
- Jiaxin Cheng, Xiao Liang, Xingjian Shi, Tong He, Tianjun Xiao, and Mu Li. Layoutdiffuse: Adapting foundational diffusion models for layout-to-image generation. *arXiv preprint arXiv:2302.08908*, 2023a.
- Yen-Chi Cheng, Hsin-Ying Lee, Sergey Tulyakov, Alexander G Schwing, and Liang-Yan Gui. Sdfusion: Multimodal 3d shape completion, reconstruction, and generation. In *Proceedings of the IEEE/CVF Conference on Computer Vision and Pattern Recognition*, pp. 4456–4465, 2023b.
- Prafulla Dhariwal and Alexander Quinn Nichol. Diffusion models beat gans on image synthesis. In *Advances in Neural Information Processing Systems*, 2021.
- Patrick Esser, Robin Rombach, and Bjorn Ommer. Taming transformers for high-resolution image synthesis. In *Proceedings of the IEEE/CVF conference on computer vision and pattern recognition*, pp. 12873–12883, 2021.
- Patrick Esser, Johnathan Chiu, Parmida Atighehchian, Jonathan Granskog, and Anastasis Germanidis. Structure and content-guided video synthesis with diffusion models. *arXiv preprint arXiv:2302.03011*, 2023.
- Rinon Gal, Yuval Alaluf, Yuval Atzmon, Or Patashnik, Amit Haim Bermano, Gal Chechik, and Daniel Cohen-or. An image is worth one word: Personalizing text-to-image generation using textual inversion. In *The Eleventh International Conference on Learning Representations*, 2022.
- Michal Geyer, Omer Bar-Tal, Shai Bagon, and Tali Dekel. Tokenflow: Consistent diffusion features for consistent video editing. *arXiv preprint arXiv:2307.10373*, 2023.
- Yuwei Guo, Ceyuan Yang, Anyi Rao, Yaohui Wang, Yu Qiao, Dahua Lin, and Bo Dai. Animatediff: Animate your personalized text-to-image diffusion models without specific tuning. *arXiv preprint arXiv:2307.04725*, 2023.

-
- William Harvey, Saeid Naderiparizi, Vaden Masrani, Christian Weilbach, and Frank Wood. Flexible diffusion modeling of long videos. *Advances in Neural Information Processing Systems*, 35: 27953–27965, 2022.
- Amir Hertz, Ron Mokady, Jay Tenenbaum, Kfir Aberman, Yael Pritch, and Daniel Cohen-Or. Prompt-to-prompt image editing with cross attention control. *arXiv preprint arXiv:2208.01626*, 2022.
- Jonathan Ho and Tim Salimans. Classifier-free diffusion guidance. *arXiv preprint arXiv:2207.12598*, 2022.
- Jonathan Ho, Ajay Jain, and Pieter Abbeel. Denoising diffusion probabilistic models. *Advances in neural information processing systems*, 33:6840–6851, 2020.
- Jonathan Ho, William Chan, Chitwan Saharia, Jay Whang, Ruiqi Gao, Alexey Gritsenko, Diederik P Kingma, Ben Poole, Mohammad Norouzi, David J Fleet, et al. Imagen video: High definition video generation with diffusion models. *arXiv preprint arXiv:2210.02303*, 2022a.
- Jonathan Ho, Tim Salimans, Alexey Gritsenko, William Chan, Mohammad Norouzi, and David J Fleet. Video diffusion models. *arXiv:2204.03458*, 2022b.
- Jonathan Ho, Tim Salimans, Alexey Gritsenko, William Chan, Mohammad Norouzi, and David J Fleet. Video diffusion models. URL <https://arxiv.org/abs/2204.03458>, 2022c.
- Bahjat Kawar, Shiran Zada, Oran Lang, Omer Tov, Huiwen Chang, Tali Dekel, Inbar Mosseri, and Michal Irani. Imagic: Text-based real image editing with diffusion models. In *Proceedings of the IEEE/CVF Conference on Computer Vision and Pattern Recognition*, pp. 6007–6017, 2023.
- Yuval Kirstain, Adam Polyak, Uriel Singer, Shahbuland Matiana, Joe Penna, and Omer Levy. Pick-a-pic: An open dataset of user preferences for text-to-image generation. *arXiv preprint arXiv:2305.01569*, 2023.
- Shaoteng Liu, Yuechen Zhang, Wenbo Li, Zhe Lin, and Jiaya Jia. Video-p2p: Video editing with cross-attention control. *arXiv preprint arXiv:2303.04761*, 2023.
- Kangfu Mei and Vishal Patel. Vidm: Video implicit diffusion models. In *Proceedings of the AAAI Conference on Artificial Intelligence*, volume 37, pp. 9117–9125, 2023.
- Chenlin Meng, Yutong He, Yang Song, Jiaming Song, Jiajun Wu, Jun-Yan Zhu, and Stefano Ermon. Sdedit: Guided image synthesis and editing with stochastic differential equations. In *International Conference on Learning Representations*, 2021.
- Ron Mokady, Amir Hertz, Kfir Aberman, Yael Pritch, and Daniel Cohen-Or. Null-text inversion for editing real images using guided diffusion models. In *Proceedings of the IEEE/CVF Conference on Computer Vision and Pattern Recognition*, pp. 6038–6047, 2023.
- Eyal Molad, Eliahu Horwitz, Dani Valevski, Alex Rav Acha, Yossi Matias, Yael Pritch, Yaniv Leviathan, and Yedid Hoshen. Dreamix: Video diffusion models are general video editors. *arXiv preprint arXiv:2302.01329*, 2023.
- Chong Mou, Xintao Wang, Liangbin Xie, Jian Zhang, Zhongang Qi, Ying Shan, and Xiaohu Qie. T2i-adapter: Learning adapters to dig out more controllable ability for text-to-image diffusion models. *arXiv preprint arXiv:2302.08453*, 2023.
- Alexander Quinn Nichol and Prafulla Dhariwal. Improved denoising diffusion probabilistic models. In *International Conference on Machine Learning*, pp. 8162–8171. PMLR, 2021.
- Alexander Quinn Nichol, Prafulla Dhariwal, Aditya Ramesh, Pranav Shyam, Pamela Mishkin, Bob McGrew, Ilya Sutskever, and Mark Chen. Glide: Towards photorealistic image generation and editing with text-guided diffusion models. In *International Conference on Machine Learning*, pp. 16784–16804. PMLR, 2022.

-
- Federico Perazzi, Jordi Pont-Tuset, Brian McWilliams, Luc Van Gool, Markus Gross, and Alexander Sorkine-Hornung. A benchmark dataset and evaluation methodology for video object segmentation. In *Proceedings of the IEEE conference on computer vision and pattern recognition*, pp. 724–732, 2016.
- Dustin Podell, Zion English, Kyle Lacey, Andreas Blattmann, Tim Dockhorn, Jonas Müller, Joe Penna, and Robin Rombach. Sdxl: Improving latent diffusion models for high-resolution image synthesis. *arXiv preprint arXiv:2307.01952*, 2023.
- Ben Poole, Ajay Jain, Jonathan T Barron, and Ben Mildenhall. Dreamfusion: Text-to-3d using 2d diffusion. In *The Eleventh International Conference on Learning Representations*, 2022.
- Chenyang Qi, Xiaodong Cun, Yong Zhang, Chenyang Lei, Xintao Wang, Ying Shan, and Qifeng Chen. Fatezero: Fusing attentions for zero-shot text-based video editing. *arXiv preprint arXiv:2303.09535*, 2023.
- Alec Radford, Jong Wook Kim, Chris Hallacy, Aditya Ramesh, Gabriel Goh, Sandhini Agarwal, Girish Sastry, Amanda Askell, Pamela Mishkin, Jack Clark, et al. Learning transferable visual models from natural language supervision. In *International conference on machine learning*, pp. 8748–8763. PMLR, 2021.
- Aditya Ramesh, Prafulla Dhariwal, Alex Nichol, Casey Chu, and Mark Chen. Hierarchical text-conditional image generation with clip latents. *arXiv preprint arXiv:2204.06125*, 2022.
- Robin Rombach, Andreas Blattmann, Dominik Lorenz, Patrick Esser, and Björn Ommer. High-resolution image synthesis with latent diffusion models. In *Proceedings of the IEEE/CVF conference on computer vision and pattern recognition*, pp. 10684–10695, 2022.
- Nataniel Ruiz, Yuanzhen Li, Varun Jampani, Yael Pritch, Michael Rubinstein, and Kfir Aberman. Dreambooth: Fine tuning text-to-image diffusion models for subject-driven generation. In *Proceedings of the IEEE/CVF Conference on Computer Vision and Pattern Recognition*, pp. 22500–22510, 2023.
- Chitwan Saharia, William Chan, Huiwen Chang, Chris Lee, Jonathan Ho, Tim Salimans, David Fleet, and Mohammad Norouzi. Palette: Image-to-image diffusion models. In *ACM SIGGRAPH 2022 Conference Proceedings*, pp. 1–10, 2022a.
- Chitwan Saharia, William Chan, Saurabh Saxena, Lala Li, Jay Whang, Emily L Denton, Kamyar Ghasemipour, Raphael Gontijo Lopes, Burcu Karagol Ayan, Tim Salimans, et al. Photorealistic text-to-image diffusion models with deep language understanding. *Advances in Neural Information Processing Systems*, 35:36479–36494, 2022b.
- Chitwan Saharia, Jonathan Ho, William Chan, Tim Salimans, David J Fleet, and Mohammad Norouzi. Image super-resolution via iterative refinement. *IEEE Transactions on Pattern Analysis and Machine Intelligence*, 45(4):4713–4726, 2022c.
- Jascha Sohl-Dickstein, Eric Weiss, Niru Maheswaranathan, and Surya Ganguli. Deep unsupervised learning using nonequilibrium thermodynamics. In *International conference on machine learning*, pp. 2256–2265. PMLR, 2015.
- Jiaming Song, Chenlin Meng, and Stefano Ermon. Denoising diffusion implicit models. In *International Conference on Learning Representations*, 2020a.
- Yang Song and Stefano Ermon. Generative modeling by estimating gradients of the data distribution. *Advances in neural information processing systems*, 32, 2019.
- Yang Song, Jascha Sohl-Dickstein, Diederik P Kingma, Abhishek Kumar, Stefano Ermon, and Ben Poole. Score-based generative modeling through stochastic differential equations. In *International Conference on Learning Representations*, 2020b.
- Junshu Tang, Tengfei Wang, Bo Zhang, Ting Zhang, Ran Yi, Lizhuang Ma, and Dong Chen. Make-it-3d: High-fidelity 3d creation from a single image with diffusion prior. *arXiv preprint arXiv:2303.14184*, 2023.

-
- MosaicML NLP Team. Introducing mpt-30b: Raising the bar for open-source foundation models, 2023. URL www.mosaicml.com/blog/mpt-30b. Accessed: 2023-06-22.
- Zachary Teed and Jia Deng. Raft: Recurrent all-pairs field transforms for optical flow. In *Computer Vision—ECCV 2020: 16th European Conference, Glasgow, UK, August 23–28, 2020, Proceedings, Part II 16*, pp. 402–419. Springer, 2020.
- Wen Wang, Kangyang Xie, Zide Liu, Hao Chen, Yue Cao, Xinlong Wang, and Chunhua Shen. Zero-shot video editing using off-the-shelf image diffusion models. *arXiv preprint arXiv:2303.17599*, 2023a.
- Xiang Wang, Hangjie Yuan, Shiwei Zhang, Dayou Chen, Jiuniu Wang, Yingya Zhang, Yujun Shen, Deli Zhao, and Jingren Zhou. Videocomposer: Compositional video synthesis with motion controllability. *arXiv preprint arXiv:2306.02018*, 2023b.
- Daniel Watson, William Chan, Ricardo Martin Brualla, Jonathan Ho, Andrea Tagliasacchi, and Mohammad Norouzi. Novel view synthesis with diffusion models. In *The Eleventh International Conference on Learning Representations*, 2022.
- Jay Zhangjie Wu, Yixiao Ge, Xintao Wang, Weixian Lei, Yuchao Gu, Wynne Hsu, Ying Shan, Xiaohu Qie, and Mike Zheng Shou. Tune-a-video: One-shot tuning of image diffusion models for text-to-video generation. *arXiv preprint arXiv:2212.11565*, 2022.
- Binxin Yang, Shuyang Gu, Bo Zhang, Ting Zhang, Xuejin Chen, Xiaoyan Sun, Dong Chen, and Fang Wen. Paint by example: Exemplar-based image editing with diffusion models. In *Proceedings of the IEEE/CVF Conference on Computer Vision and Pattern Recognition*, pp. 18381–18391, 2023a.
- Shuai Yang, Yifan Zhou, Ziwei Liu, and Chen Change Loy. Rerender a video: Zero-shot text-guided video-to-video translation. *arXiv preprint arXiv:2306.07954*, 2023b.
- Lvmin Zhang and Maneesh Agrawala. Adding conditional control to text-to-image diffusion models. *arXiv preprint arXiv:2302.05543*, 2023.
- Yuxin Zhang, Nisha Huang, Fan Tang, Haibin Huang, Chongyang Ma, Weiming Dong, and Changsheng Xu. Inversion-based style transfer with diffusion models. In *Proceedings of the IEEE/CVF Conference on Computer Vision and Pattern Recognition*, pp. 10146–10156, 2023.
- Min Zhao, Rongzhen Wang, Fan Bao, Chongxuan Li, and Jun Zhu. Controlvideo: Adding conditional control for one shot text-to-video editing. *arXiv preprint arXiv:2305.17098*, 2023.

SUPPLEMENTARY OF COHERENT VIDEO-TO-VIDEO TRANSFER USING SYNTHETIC DATASETS

A INSTRUCTION FOR ZERO-SHOT MPT DATA GENERATION:

The instruction for MPT comprises three parts. The first is the task description which delineates the objectives for the bot.

You are a bot to generate synthetic text data for generating video clip. You will creatively generate paired prompt triplet for synthetic data generation for video clip. You will be given an input prompt and you should return the edit prompt and output prompt. The output prompt reflects the sentence after applying edit prompt on the input prompt. Ensure that the prompt are proper for generating video clip (i.e. prompt should describe a scene).

Successful editing do changing the main subject, modifying the context or setting or altering the artistic style.

Here are some examples of editing that are likely to success (do not limit to the verb used in the follow. You must be creative and the editing should be diverse):

Edit of Landscape:

Edit: Convert the cityscape to a seascape.

Edit: Turn the desert scene into a lush forest.

Replacement of Characters:

Edit: Replace the cowboys with astronauts.

Edit: Turn the group of children into a group of elderly people.

Edit of Time:

Edit: Switch the night scene to a day scene.

Edit: Transform the contemporary setting into a medieval setting.

Addition of Significant Elements:

Edit: Add a full moon to the clear sky.

Edit: Include a rainbow in the cloudy scene.

Edit of Weather or Season:

Edit: Make the sunny day into a snowfall.

Edit: Transform the summer scene into autumn.

Edit the Action or Activity:

Edit: Change the soccer game to a ballet performance.

Edit: Replace the cooking scene with a gardening scene.

Edit of Artistic Style:

Edit: Make it look like a watercolor painting.

Edit: It is now in the style of Van Gogh. (do not only use Van
→ Gogh)

The subsequent phase of the instruction involves presenting MPT with five randomly selected examples from the LAION-IPTP dataset. These samples have been previously successful in generating paired prompts that meet the CLIP filter criteria. The depiction below illustrates this process:

Here are some success examples (please be creative and not limited
→ to examples)

Input: Graham Wands - George Square, Glasgow, watercolour
Edit: Turn the watercolour into a pencil sketch
Output: Graham Wands - George Square, Glasgow, pencil sketch

Input: Pierre de Clausade, (French, 1910-1976), Winter at the Lake
Edit: make it a sunset
Output: Pierre de Clausade, (French, 1910-1976), Sunset at the
→ Lake

Input: Rex Beanland, Charing Cross, watercolour, 9 12
Edit: make it an oil painting
Output: Rex Beanland, Charing Cross, oil painting, 9 12

Input: Mark Van Crombrugge, Old Milk Bottle and Grapes, oil, 31 x
→ 59.
Edit: Make the bottle transparent.
Output: Mark Van Crombrugge, Transparent Old Milk Bottle, oil, 31
→ x 59.

Input: ""Large Original Oil painting on canvas. Beautiful
→ portrait of a woman 24x24""
Edit: make the woman a cat
Output: ""Large Original Oil painting on canvas. Beautiful
→ portrait of a cat 24x24""

Finally, MPT is provided with video captions from the WebVid dataset that are designated for processing. This marks the initiation of the generation process for novel, paired prompts.

Generate triplet for following inputs:

Merida, mexico - may 23, 2017: tourists are walking on a roadside
→ near catholic church in the street of mexico at sunny summer
→ day.

Fun clown - 3d animation

Happy family using laptop on bed at home

11th march 2017. nakhon pathom, thailand. devotees goes into a
→ trance at the wai khru ceremony at wat bang phra temple. what
→ bang phra is famous for its magically charged tattoos and
→ amulets.

Decorate with pineapple sweet cake roll.

Beautiful lake aerial view

Frankfurt, germany-circa 2013:traffic with skyscrapers in
→ background at night along the river main in frankfurt, time
→ lapse

Young positive couple laughing in the backyard in front of the
→ large house under falling snow. bearded man and attractive
→ woman in warm clothes have winter fun. the guy showing thumb
→ up

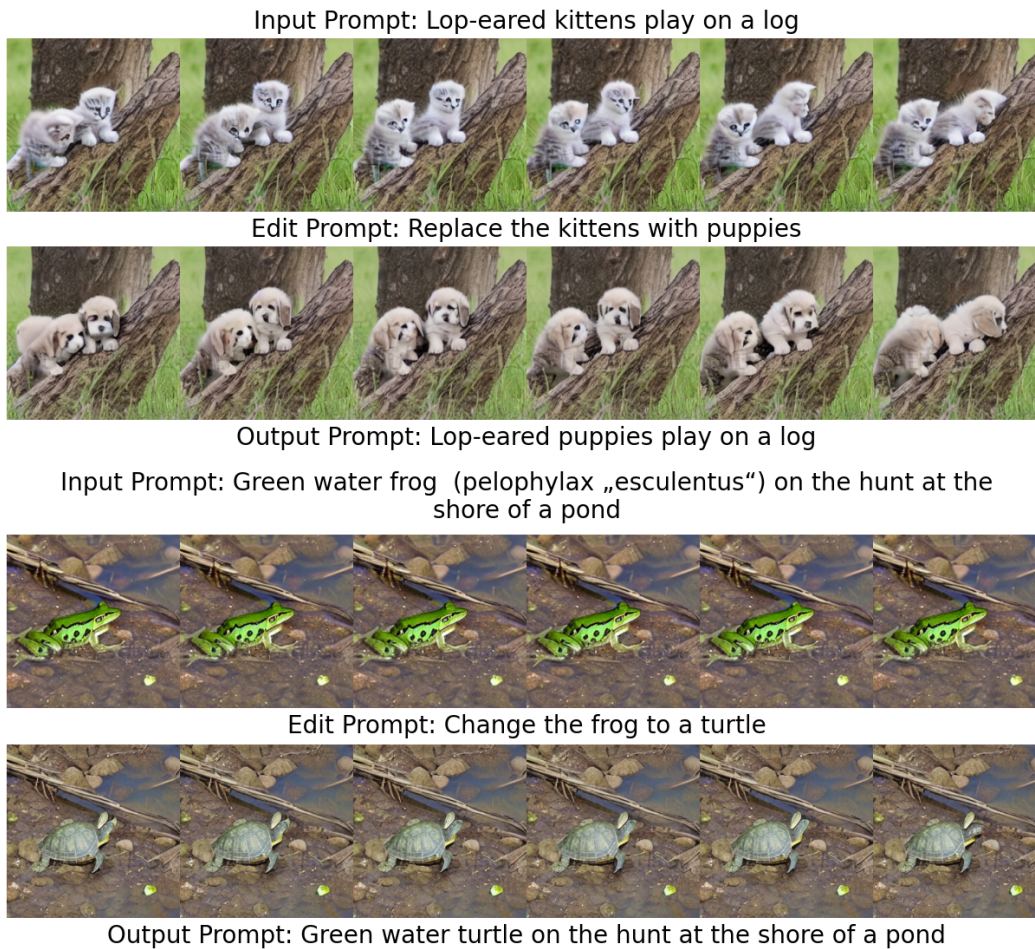


Figure 5: Visualization of synthetic samples produced by the data generation pipeline in Section 3. Each sample contains two generated videos: the upper one represents the input prompt, while the lower one depicts the output prompt. The actual videos comprise 16 frames while 6 subsampled frames are displayed here for brevity.

Broadcast twinkling squared diamonds, multi color, abstract,
 → loopable, 4k

Wheat harvesting. combine harvester gathers the wheat crop on the
 → field.

B VISUALIZATION OF SYNTHETIC VIDEO DATASET

In Section 3, we introduce a pipeline designed to produce synthetic paired videos. Further visual demonstrations of these results can be found in Figures 5 and 6. The generated paired videos maintain a similar structure, and the editing can showcase the edit prompt.

C LONG VIDEO SAMPLING DETAIL ILLUSTRATION AND EXAMPLES

In Section 4.4, we addressed the challenge of ensuring consistency across different batches when sampling long videos, particularly when each batch is processed separately. This section introduces an illustrative explanation of the Long Video Sampling Correction (LVSC) method in Figure 7. In

Input Prompt: Chicago, illinois - 2010: this is a sculpture of a lion located in front of the art institute of chicago on michigan avenue. this lion can be seen in chicago movies like ferris bueller's day off.



Edit Prompt: Replace the lion with a dragon



Output Prompt: Chicago, illinois - 2010: this is a sculpture of a dragon located in front of the art institute of chicago on michigan avenue.

Input Prompt: Honey bees on the pink flowers of a tree peony collect honey and pollen.



Edit Prompt: The pink flowers are replaced with sunflowers.



Output Prompt: Honey bees on the sunflowers collect honey and pollen.

Input Prompt: Woman is eating pizza at home



Edit Prompt: Replace pizza with sushi



Output Prompt: Woman is eating sushi at home

Figure 6: Visualization of synthetic samples produced by the data generation pipeline in Section 3. Each sample contains two generated videos: the upper one represents the input prompt, while the lower one depicts the output prompt. The actual videos comprise 16 frames while 6 subsampled frames are displayed here for brevity.

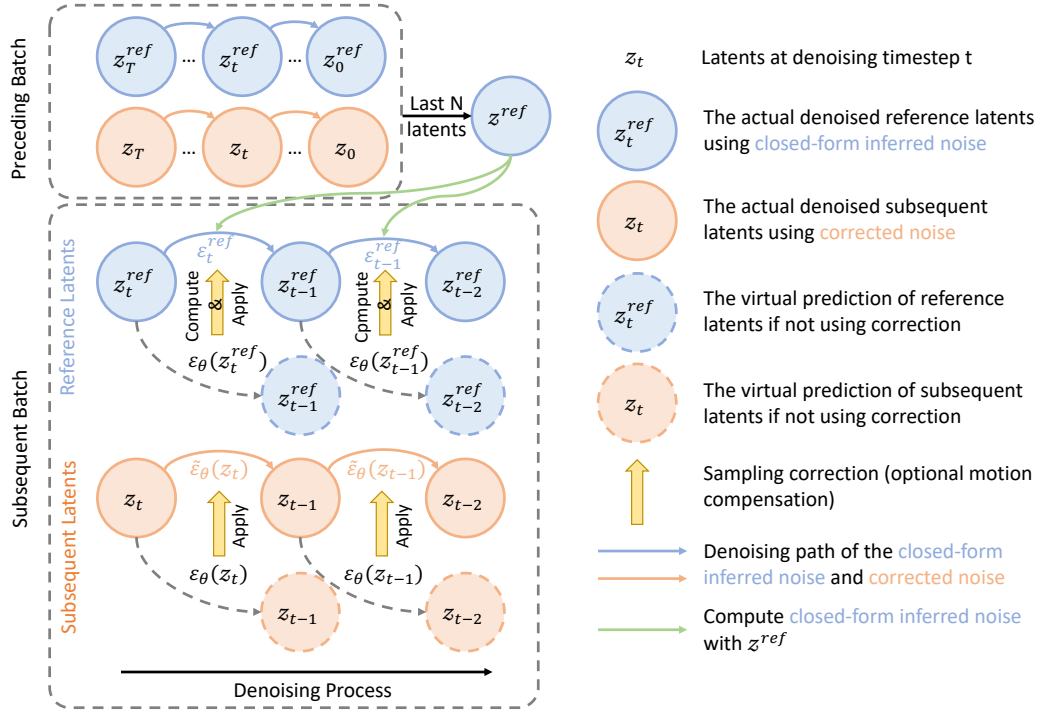


Figure 7: Schematic of Long Video Sampling Correction (LVSC) mechanism. The diagram illustrates the interaction between reference latents from a preceding batch and subsequent latents during the denoising process. The closed-form inferred noise (Equation (4)) is computed for the N reference latents (shown in blue), which then guides the correction of the actual denoised subsequent latents (shown in orange).

LVSC, there are N overlapping reference frames between two consecutive batches, but this method transcends a basic sliding window technique. Instead of allowing the editing model unrestricted freedom in transferring edits, the reference frames guide the appearance of subsequent frames during the editing process.

Additionally, we present a visual comparison to demonstrate the impact of LVSC. Figure 8 contrasts the results with and without LVSC implementation. This comparison clearly shows the lack of continuity in the sampled frames between batches when LVSC is not applied. In contrast, employing LVSC achieves noticeable consistency, aligning the first frame of a subsequent batch with the last frame of the previous batch.

D EFFECT OF MOTION COMPENSATION IN LONG VIDEO SAMPLING CORRECTION

In our experiments, we observed that the presence of holistic camera motion could degrade the transfer results of subsequent batches processed by the LVSC model (see red boxes in Figure 9). This degradation arises because the same regions across different frames require consistent score corrections. In other words, score corrections should “travel” with the regions affected by camera movement, ensuring that identical corrections are applied to the same areas regardless of motion. To address this issue, we introduce a motion compensation strategy. Specifically, we first employ the RAFT flow estimator Teed & Deng (2020) to compute the optical flow between each reference frame and the remaining frames in subsequent batches. The original equation for LVSC (Equation (5)) is then modified as follows:

$$\tilde{\varepsilon}_\theta(z_t)[:, m] = \varepsilon_\theta(z_t)[:, m] + \left(\frac{1}{N} \sum_{i=1}^N o(\varepsilon_t^{ref}[:, i]), i \rightarrow m) - \varepsilon_\theta(z_t)[:, m] \right) \quad (6)$$

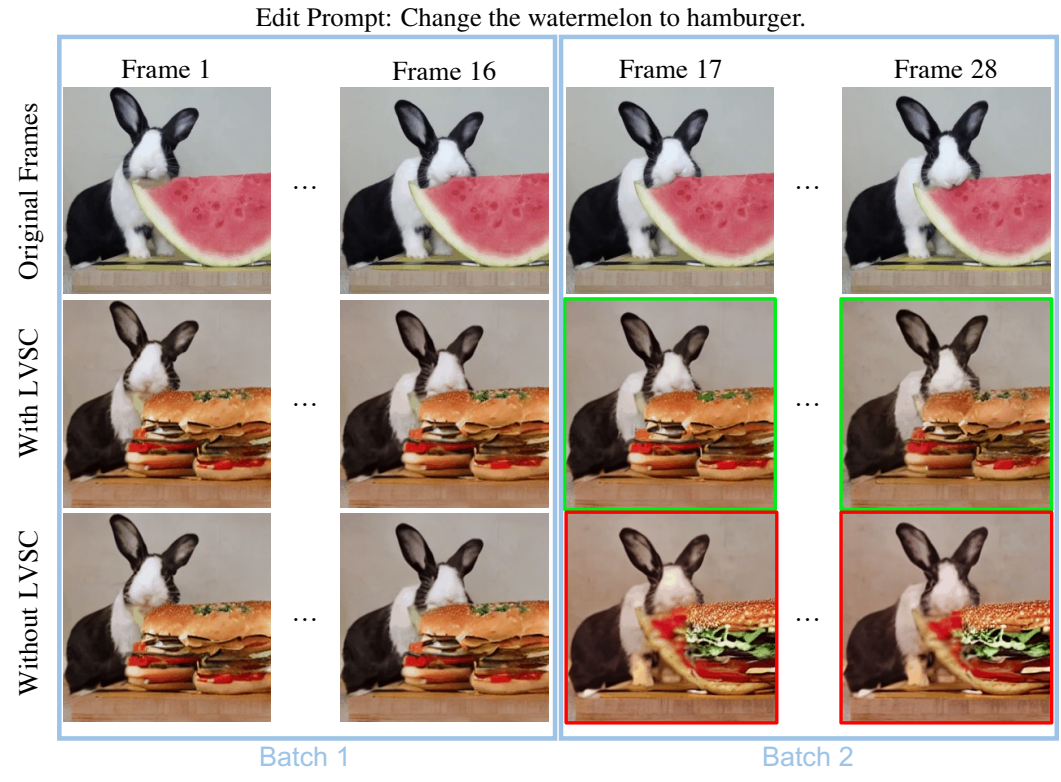


Figure 8: In the process of video sampling, we utilize a batch size of 16. The 17th to 28th frames in the video are processed in the second batch, and they reference the last four sampled frames from the preceding batch. By employing the Long Video Sampling Correction (LVSC), we can ensure the content consistency between sampled frames across different batches (green boxes in the figure). In contrast, sampling two batches separately may lead to inconsistencies at the boundaries where the batches change (red boxes in the figure).

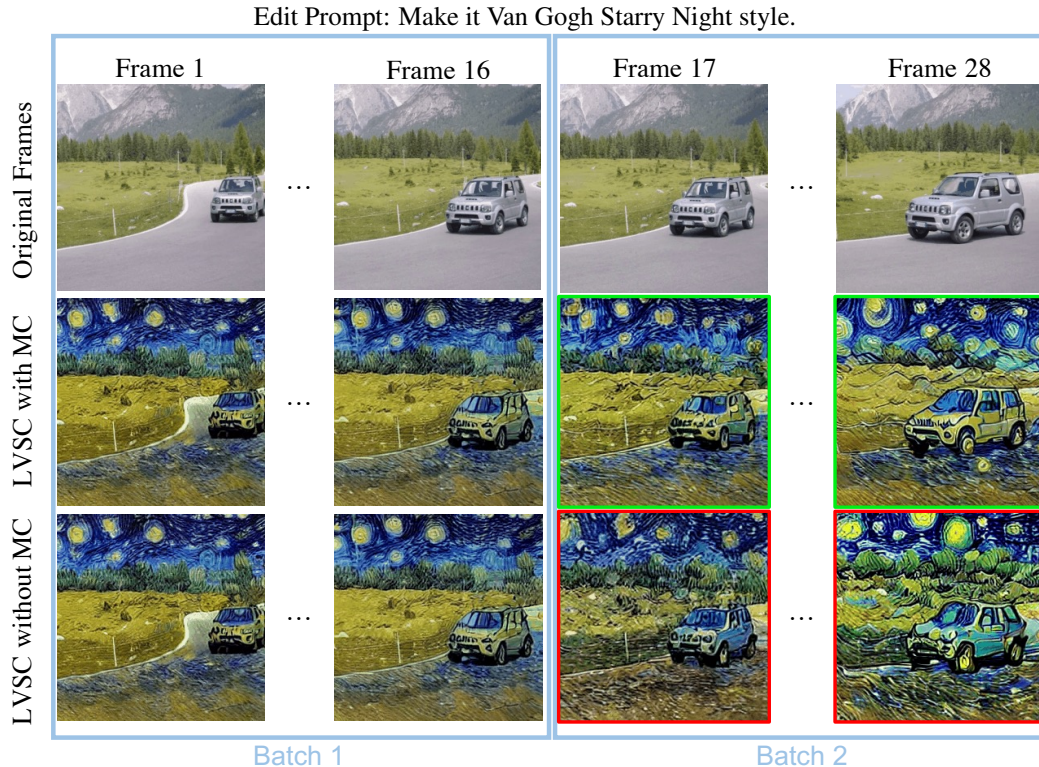


Figure 9: When the video exhibits extensive camera motion, the LVSC model without motion compensation (LVSC without MC) suffers significant quality degradation, particularly in frames from subsequent batches (red boxes in the figure). Incorporating motion compensation (LVSC with MC) substantially improves frame consistency with the reference and maintains high transfer quality, even when the camera view changes dramatically in later batches (green boxes in the figure).

Here, $m = [1, 2, \dots, M]$ represents the indices of frames in the subsequent batches, which contain a total of M frames, $o(\cdot, i \rightarrow m)$ is a warping function that uses optical flow to align the i -th reference frame with the m -th frame in the subsequent batch. This modification ensures better transfer quality by making the score corrections to be aware of camera movement. The green boxes in Figure 9 reveal that applying motion compensation significantly enhances content consistency and overall quality. This improvement is particularly noticeable in the last few frames of the subsequent batches.

E EFFECT OF SAMPLING HYPERPARAMETERS AND PICKING CRITERIA

In our experiments, we observed that the video CFG and resolution have a greater impact on the generated video than the text CFG. To streamline the parameter search process, we thus focus solely on picking the video CFG and resolution, effectively reducing the search space. Detailed visual effects of the hyperparameter choices are provided in Figure 10. We opt for PickScore Kirstain et al. (2023) as our automated selection criterion. Our choice is motivated by the fact that PickScore aligns more closely with human perception compared to the CLIP score, as indicated in Kirstain et al. (2023).

F QUALITATIVE COMPARISONS

We provide qualitative comparisons with baselines in Figures 11 to 19

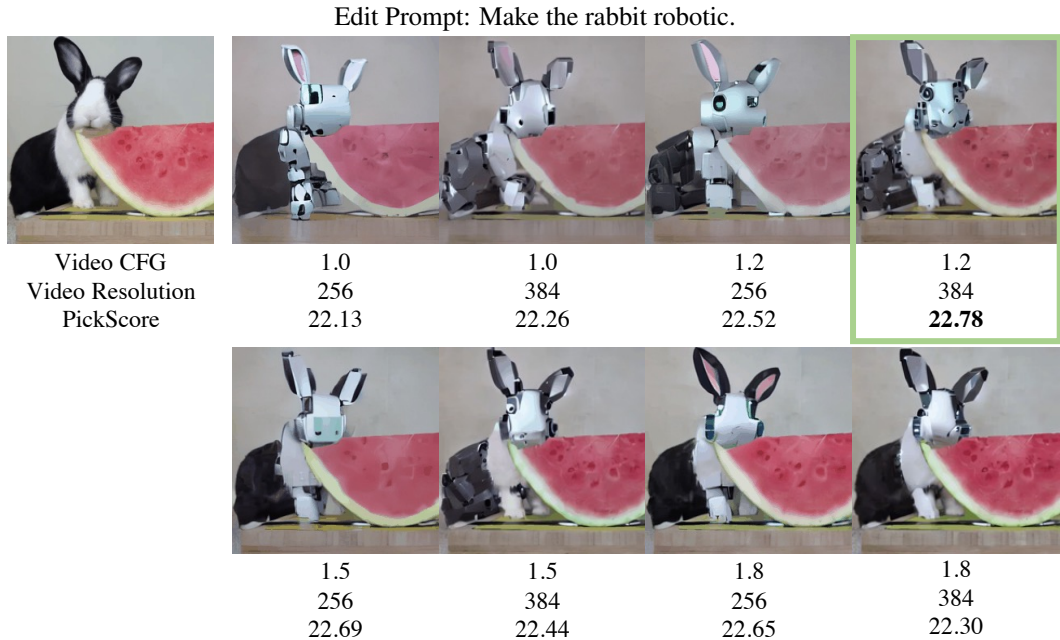


Figure 10: During sampling, the interplay between the scale of image classifier-free guidance (CFG) and image size can significantly influence the transfer result. In our evaluation, we sample videos by employing various combinations of CFG scales and resolutions, utilizing the average PickScore across all frames as the selection metric. The video with the highest PickScore is designated as the final transfer result. As indicated by the green box in the figure, the chosen video and its corresponding hyperparameters bear the highest PickScore, thereby making it the final selection.

G FAILURE CASES

Our model, InsV2V, occasionally encounters challenges in video transfer, particularly when the object of interest is difficult to detect. Such difficulties arise when the object is positioned close to the video’s edge, is unusually small or large, or is partially obscured. These scenarios can lead to the object either vanishing in the edited video or exhibiting inconsistent appearances.

For instance, as depicted in Figure 20, when a person is situated near the frame’s border and occupies a small area, InsV2V struggles to maintain the person’s structural integrity, resulting in their disappearance from the transferred video. However, when the person moves away from the border, InsV2V can recognize them again, but with a notably altered appearance.

Figure 21 presents another scenario where the object, in this case, the front part of a truck, is only partially visible in certain frames. While InsV2V can accurately transfer the image when the truck is fully visible, it misinterprets the partially visible truck as a car’s front, leading to inconsistent results in the transferred video.

In summary, when object detection is hindered due to size, positioning, or occlusion, InsV2V may not deliver satisfactory transfer results.



Figure 11: Swans gliding over a lake. → Pink flamengos gliding over a lake.

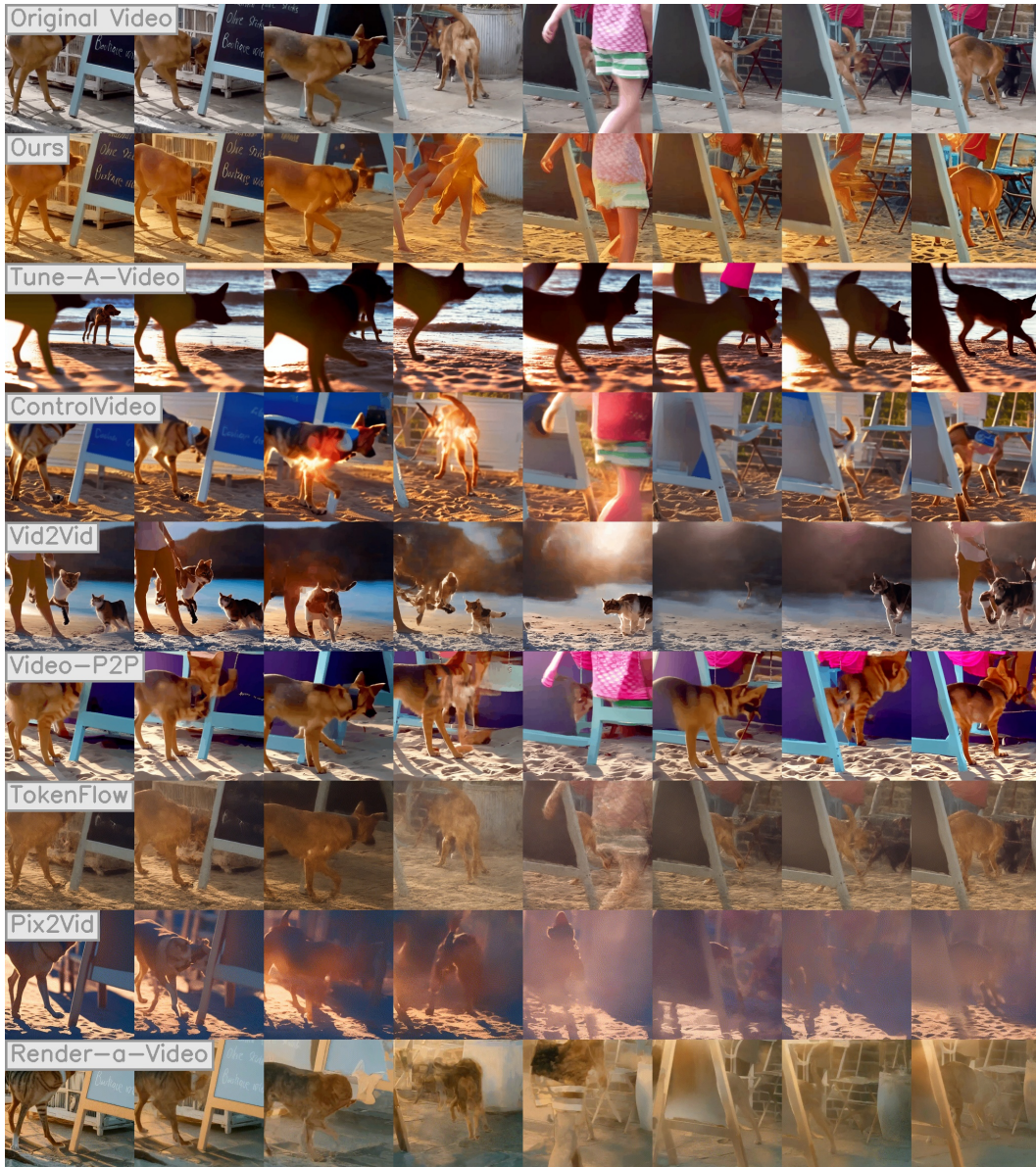


Figure 12: A cat and a dog playing on the street while a girl walks around them.
 → A cat and a dog playing on the beach while a girl walks around them, **golden hour lighting**.

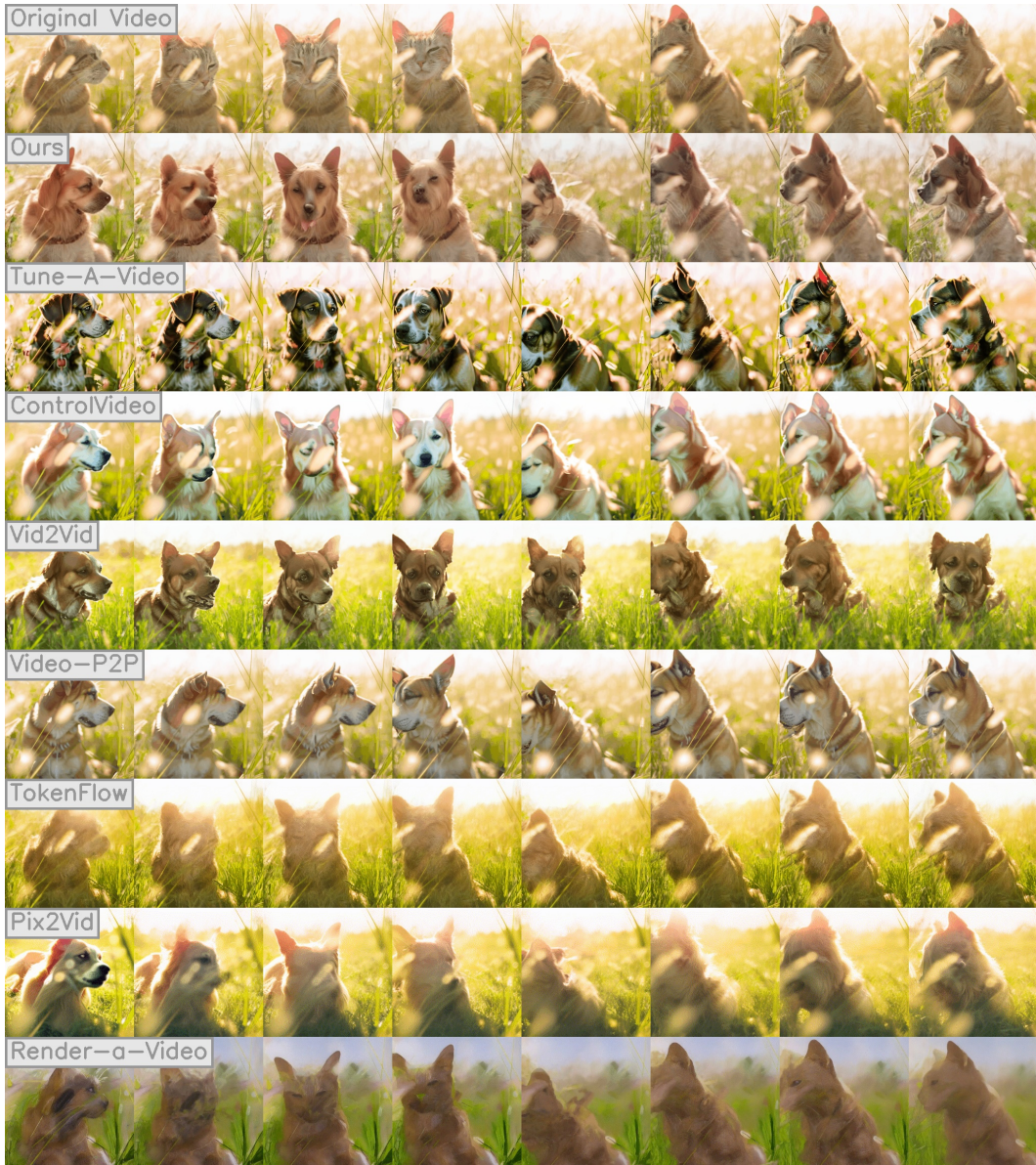


Figure 13: A **cat** in the grass in the sun. → A **dog** in the grass in the sun.

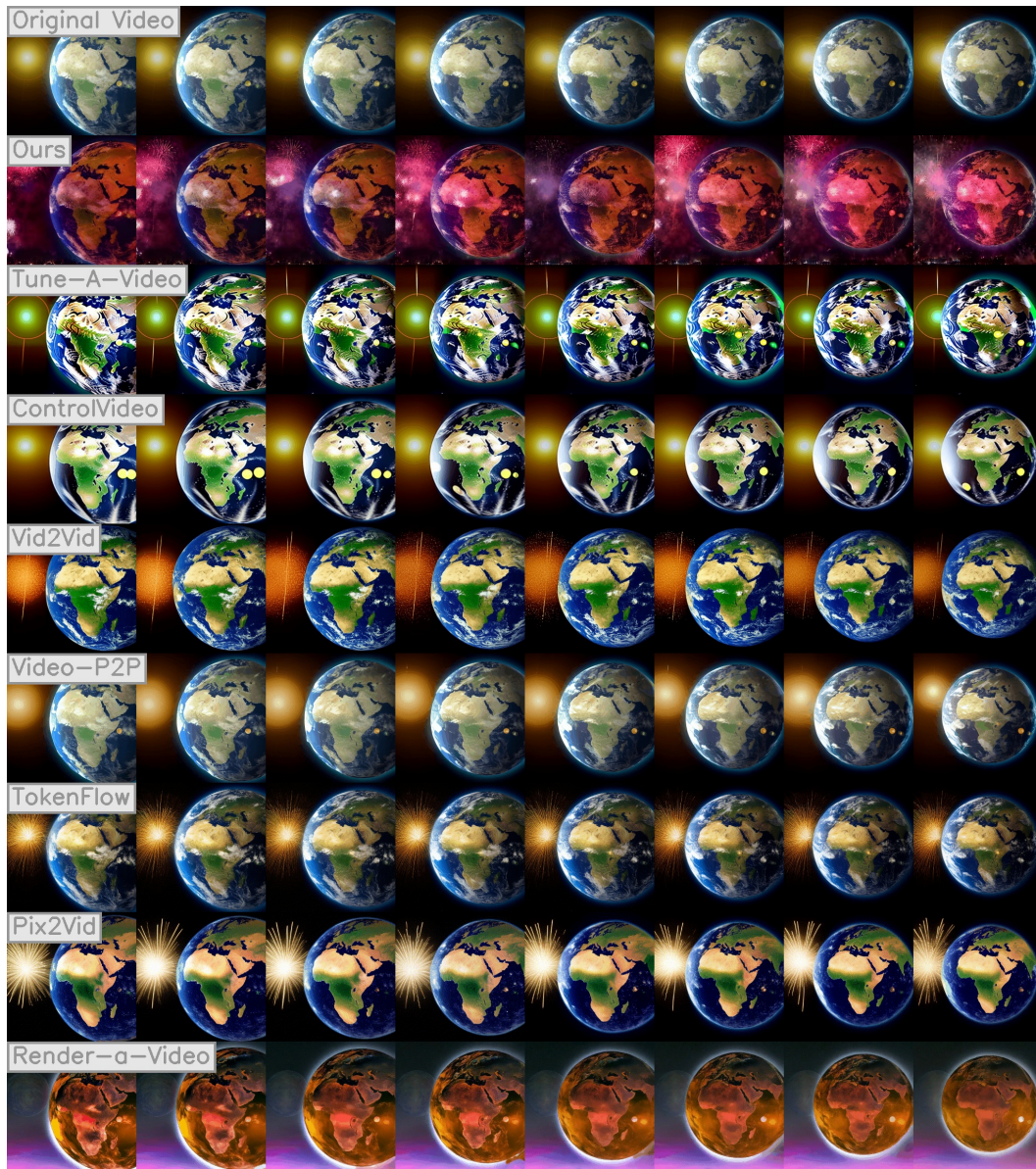


Figure 14: Full view of the Earth as it moves slowly **toward the sun**.
→ Full view of the Earth as it moves slowly **through a fireworks display**.

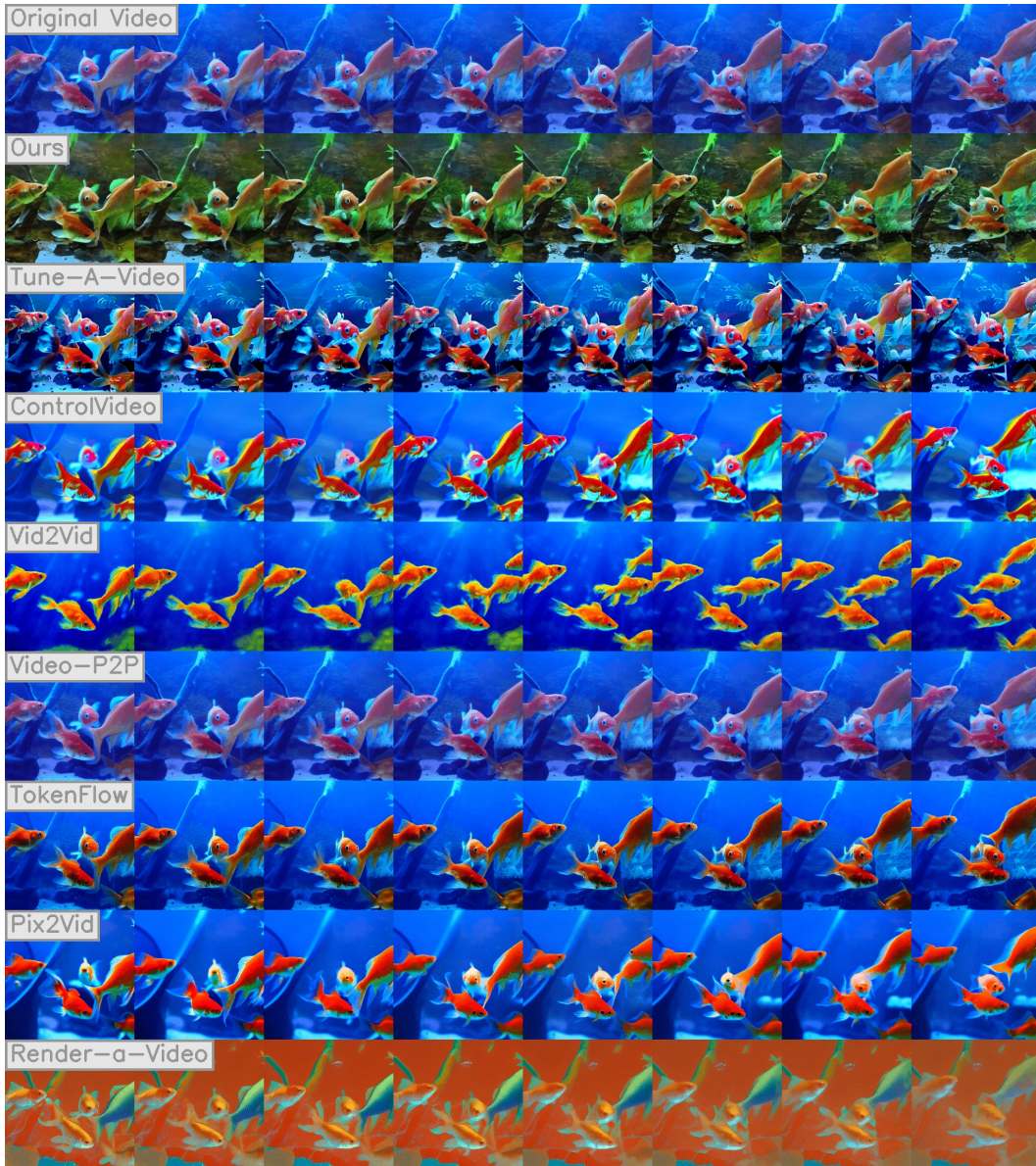


Figure 15: Several goldfish swim in a **tank**. → Several goldfish swim in a **pond**.



Figure 16: A static shot of red roses in sunlight, gently swaying in the breeze.
→ A static shot of red roses in sunlight, gently swaying in the breeze, **origami style**.



Figure 17: A Delta Airlines aircraft descends onto the runway during a cloudless morning.
→ A **brightly colored cyberpunk aircraft** descends onto the runway during a cloudless morning, **with a bustling cityscape in the background.**

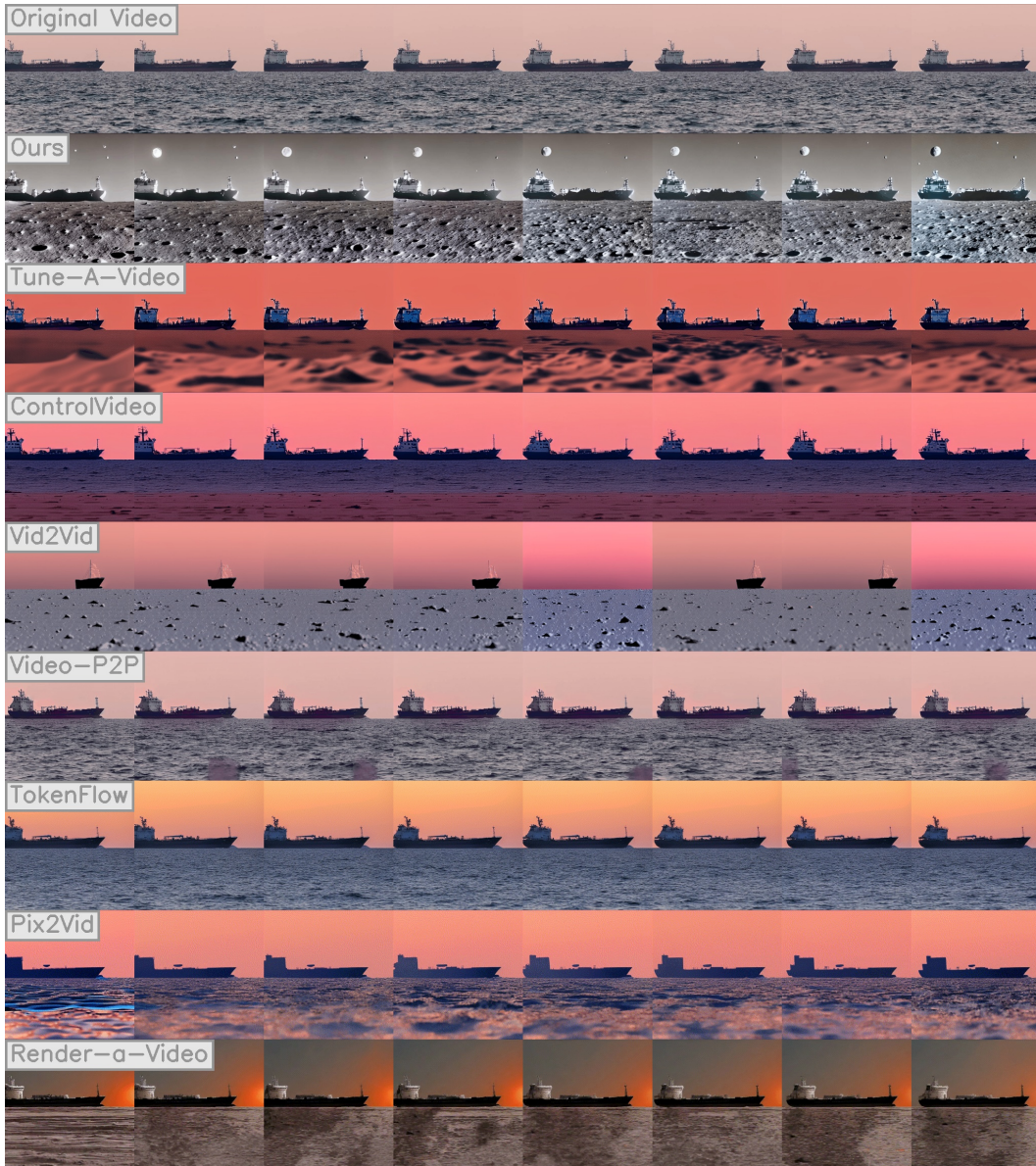


Figure 18: A ship sails on the **sea**. → A ship sails on the **lunar surface**.

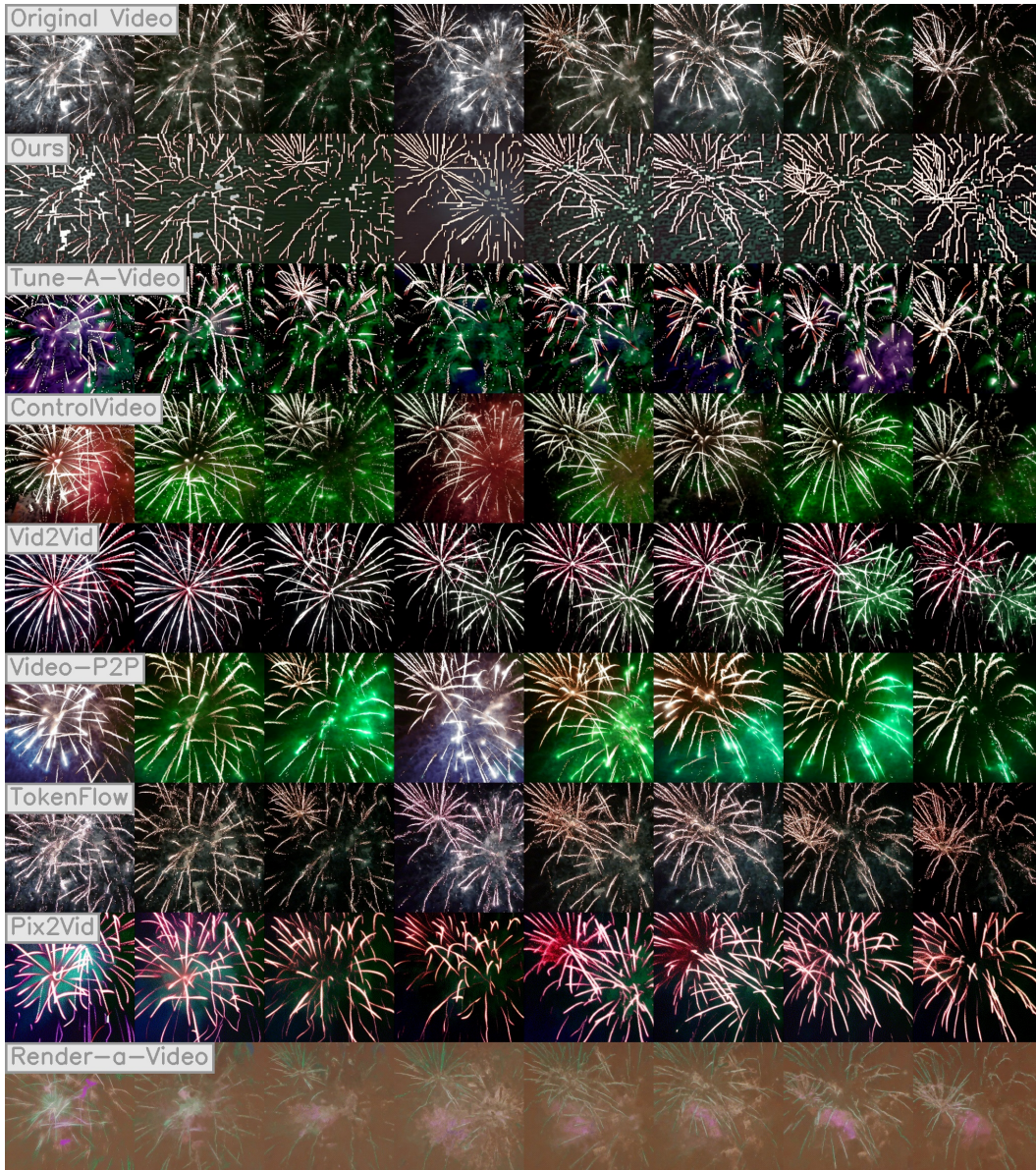


Figure 19: A colourful fireworks display in the night sky.
→ A colourful fireworks display in the night sky, **8-bit pixelated**.

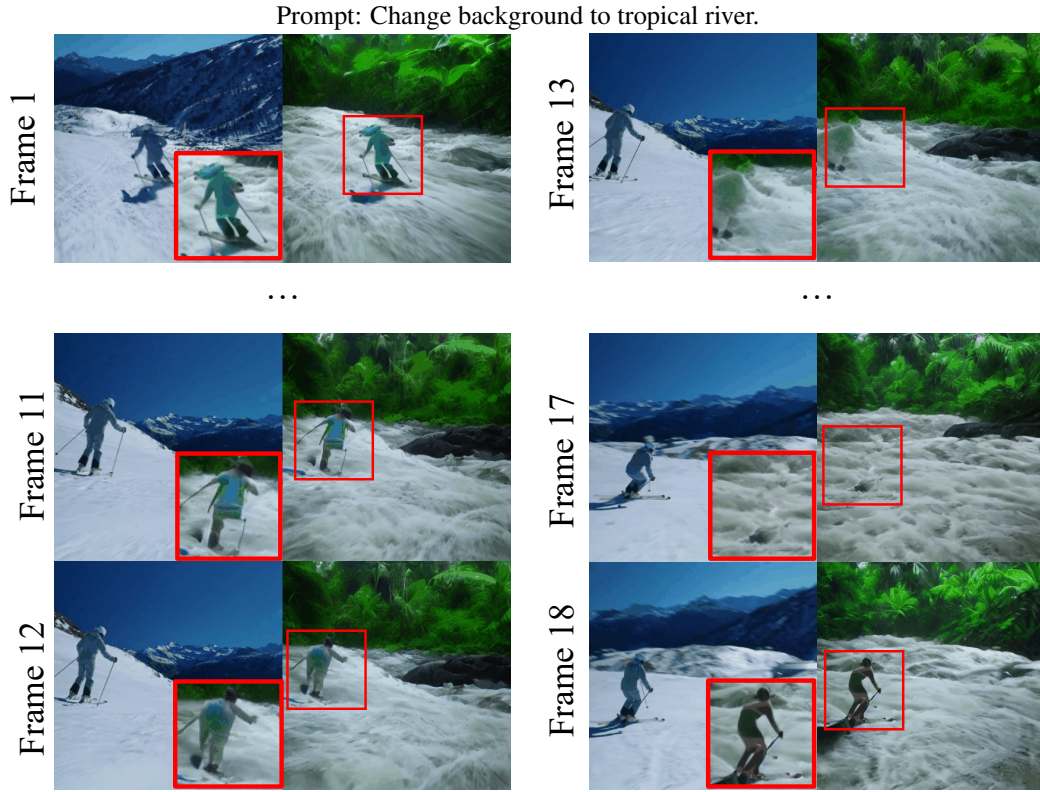


Figure 20: Illustration of a failure case where InsV2V struggles to maintain the structure of a person located near the video's edge and occupying a small area, resulting in the disappearance of the person from the transferred video.

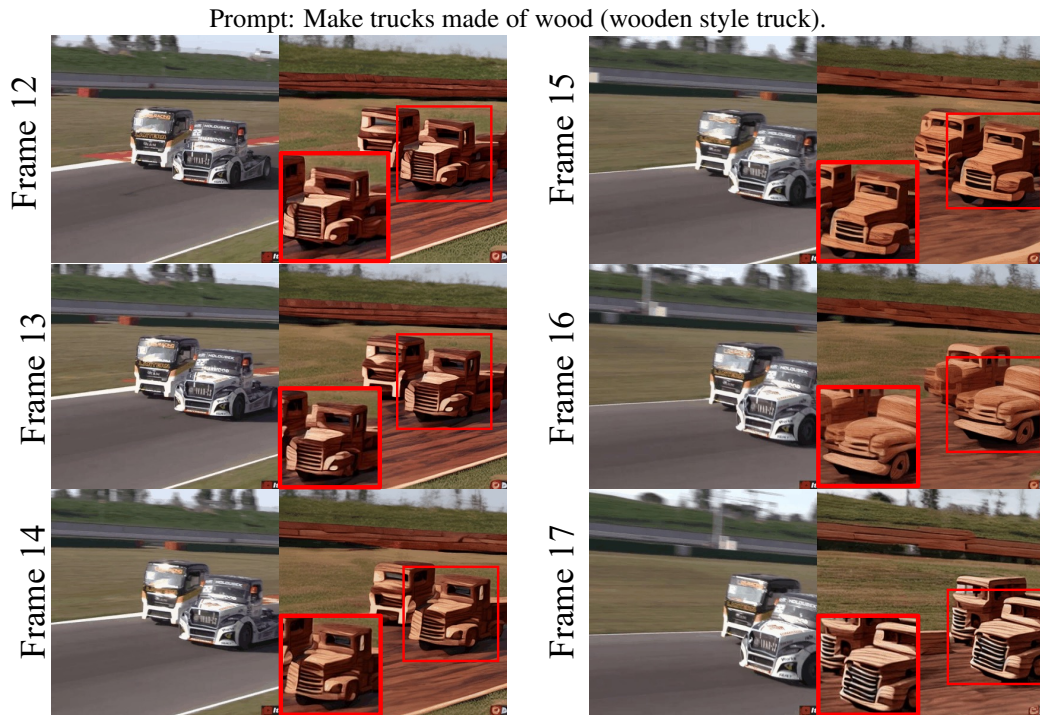


Figure 21: Demonstration of a failure scenario in InsV2V where a partially visible truck is misidentified as a car's front, leading to inconsistent transfer results in the edited video.